Journal of
Mechanics of
Materials and Structures

STATIC BENDING ANALYSIS OF LAMINATED CYLINDRICAL PANELS WITH VARIOUS BOUNDARY CONDITIONS USING THE DIFFERENTIAL CUBATURE METHOD

S. Mahmoud Mousavi and Mohamad M. Aghdam

Volume 4, Nº 3 March 2009

mathematical sciences publishers

JOURNAL OF MECHANICS OF MATERIALS AND STRUCTURES
Vol. 4, No. 3, 2009

STATIC BENDING ANALYSIS OF LAMINATED CYLINDRICAL PANELS WITH VARIOUS BOUNDARY CONDITIONS USING THE DIFFERENTIAL CUBATURE METHOD

S. MAHMOUD MOUSAVI AND MOHAMAD M. AGHDAM

This paper deals with the application of the differential cubature method (DCM) to the bending analysis of laminated cylindrical panels. Symmetric and unsymmetric laminate, with various combinations of clamped, simply supported and free boundary conditions, are considered, with either uniform or sinusoidal transversely distributed loads. Using first-order shear deformation theory, fifteen first-order partial differential equations are obtained, containing as many unknowns in terms of displacements, rotations, moments, and forces. Comparison of the results obtained by DCM shows very good agreement with those of other numerical and analytical methods, with decreased computational effort. Further, in this method, a free boundary condition and unsymmetric laminates do not violate the accuracy of the results.

A list of symbols can be found starting on page 519.

1. Introduction

Considerable research has been conducted to investigate the response of thin/thick laminated cylindrical panels, as one of the fundamental parts of engineering structures. Since only particular elasticity problems can be studied using analytical methods, numerical techniques have been developed to obtain solutions for different structural components subjected to various types of loading and boundary conditions. Among the methods employed we mention the finite difference [Smith 2000], finite element [Qatu and Algothani 1994; Reddy 2004], boundary element [Jianqiao 1988], dynamic relaxation [Ramesh and Krishnamoorthy 1995], and extended Kantorovich methods [Yuan et al. 1998; Alijani et al. 2008], meshless methods [Alavi et al. 2006], and the differential quadrature (DQ) [Artioli et al. 2005], generalized differential quadrature (GDQ) [Aghdam et al. 2006], and differential cubature methods (DCM) [Civan 1994; Liew and Liu 1997; 1998; Teo and Liew 2002; Wu and Liu 2005].

In the literature of the static bending analysis of shells and plates, the free boundary condition has been a major problem and usually the methods lose their accuracy when there is even one free edge. Although this is more of a problem with analytical methods than numerical ones, only a few numerical methods — such as GDQ [Aghdam et al. 2006], FEM [Bhaskar and Varadan 1991], and state space [Khdeir et al. 1989] — can be assumed safe for dealing with static problems involving shells and plates with free edges. Naturally, then, the development of new methods usable for unsymmetric shells with some free edges is a desirable goal.

The DCM was presented in [Civan 1994] as an efficient procedure to obtain solutions for partial differential equations with a relatively small number of grid points and less computational effort. However, reported applications of the DCM in the open literature are restricted to analyses of plates, including

Keywords: cylindrical panel, unsymmetric laminates, differential cubature method, bending analysis.

bending [Liew and Liu 1997; 1998; Teo and Liew 2002] and vibration [Wu and Liu 2005]. Nothing was found in the open literature for other structural elements, such as shells and panels.

Here we perform a bending analysis of laminated cylindrical panels with various loading boundary conditions using the DCM. The complete form of the governing partial differential equations of the problem based on first-order shear deformation theory is considered. All panel variables including displacements, rotations, moment, and force resultants are presented in the governing equations. The presence of all variables provides an easy way to satisfy different boundary conditions.

The solution to the governing equations provides direct predictions of all variables with the same order of accuracy. Both governing equations and solution domain are discretized using DCM. As with most other numerical techniques, this yields a system of linear algebraic equations. Comparison of the predictions for stress resultants and displacement components shows very good agreement with results of other analytical and numerical techniques. The lamination sequence of the examples are symmetric, unsymmetric, cross-ply and angle-ply. There is no restriction to using this method for panels with free edges.

2. Governing equations

As a test case for the capabilities of the DCM and the accuracy of its results, we consider a moderately thick laminated cylindrical shell panel with length a, thickness h, and mid-surface radius R (Figure 1). Using the principle of minimum potential energy and the assumptions of first-order shear deformation theory (FSDT), one obtains the fifteen first-order PDEs listed in Table 1, which constitute the general form of the governing partial differential equations of the problem; see [Toorani and Lakis 2000] for details. (These governing equations have been used and verified in some recent surveys such as [Aghdam et al. 2006; Toorani and Lakis 2001].)

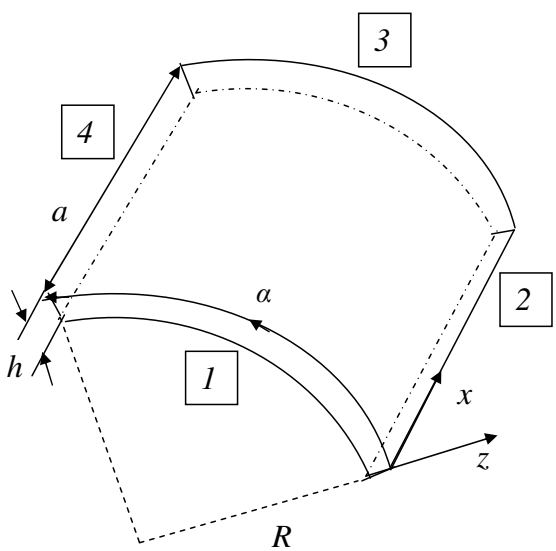

Figure 1. Shell geometry and coordinate system.

$$N_{xx} - G_{11}\frac{\partial u_x}{\partial x} - G_{16}\frac{\partial u_\theta}{\partial x} - \frac{A_{12}}{R}\left(w + \frac{\partial u_\theta}{\partial \theta}\right) - \frac{A_{16}}{R}\frac{\partial u_x}{\partial \theta} - H_{11}\frac{\partial \beta_x}{\partial x} - H_{16}\frac{\partial \beta_\theta}{\partial x} - \frac{B_{12}}{R}\frac{\partial \beta_\theta}{\partial \theta} - \frac{B_{16}}{R}\frac{\partial \beta_x}{\partial \theta} = 0,$$

$$N_{x\theta} - G_{61}\frac{\partial u_x}{\partial x} - G_{66}\frac{\partial u_\theta}{\partial x} - \frac{A_{62}}{R}\left(w + \frac{\partial u_\theta}{\partial \theta}\right) - \frac{A_{66}}{R}\frac{\partial u_x}{\partial \theta} - H_{61}\frac{\partial \beta_x}{\partial x} - H_{66}\frac{\partial \beta_\theta}{\partial x} - \frac{B_{62}}{R}\frac{\partial \beta_\theta}{\partial \theta} - \frac{B_{66}}{R}\frac{\partial \beta_x}{\partial \theta} = 0,$$

$$N_{\theta\theta} - A_{21}\frac{\partial u_x}{\partial x} - A_{26}\frac{\partial u_\theta}{\partial x} - \frac{G'_{22}}{R}\left(w + \frac{\partial u_\theta}{\partial \theta}\right) - \frac{G'_{26}}{R}\frac{\partial u_x}{\partial \theta} - B_{21}\frac{\partial \beta_x}{\partial x} - B_{26}\frac{\partial \beta_\theta}{\partial x} - \frac{H'_{22}}{R}\frac{\partial \beta_\theta}{\partial \theta} - \frac{H'_{26}}{R}\frac{\partial \beta_x}{\partial \theta} = 0,$$

$$N_{\theta x} - A_{61}\frac{\partial u_x}{\partial x} - A_{66}\frac{\partial u_\theta}{\partial x} - \frac{G'_{62}}{R}\left(w + \frac{\partial u_\theta}{\partial \theta}\right) - \frac{G'_{66}}{R}\frac{\partial u_x}{\partial \theta} - B_{61}\frac{\partial \beta_x}{\partial x} - B_{66}\frac{\partial \beta_\theta}{\partial x} - \frac{H'_{62}}{R}\frac{\partial \beta_\theta}{\partial \theta} - \frac{H'_{66}}{R}\frac{\partial \beta_x}{\partial \theta} = 0,$$

$$M_{xx} - H_{11}\frac{\partial u_x}{\partial x} - H_{16}\frac{\partial u_\theta}{\partial x} - \frac{B_{12}}{R}\left(w + \frac{\partial u_\theta}{\partial \theta}\right) - \frac{B_{16}}{R}\frac{\partial u_x}{\partial \theta} - J_{11}\frac{\partial \beta_x}{\partial x} - J_{16}\frac{\partial \beta_\theta}{\partial x} - \frac{D_{12}}{R}\frac{\partial \beta_\theta}{\partial \theta} - \frac{D_{16}}{R}\frac{\partial \beta_x}{\partial \theta} = 0,$$

$$M_{x\theta} - H_{61}\frac{\partial u_x}{\partial x} - H_{66}\frac{\partial u_\theta}{\partial x} - \frac{B_{62}}{R}\left(w + \frac{\partial u_\theta}{\partial \theta}\right) - \frac{B_{66}}{R}\frac{\partial u_x}{\partial \theta} - J_{61}\frac{\partial \beta_x}{\partial x} - J_{66}\frac{\partial \beta_\theta}{\partial x} - \frac{D_{62}}{R}\frac{\partial \beta_\theta}{\partial \theta} - \frac{D_{66}}{R}\frac{\partial \beta_x}{\partial \theta} = 0,$$

$$M_{\theta\theta} - B_{21}\frac{\partial u_x}{\partial x} - B_{26}\frac{\partial u_\theta}{\partial x} - \frac{H'_{22}}{R}\left(w + \frac{\partial u_\theta}{\partial \theta}\right) - \frac{H'_{26}}{R}\frac{\partial u_x}{\partial \theta} - D_{21}\frac{\partial \beta_x}{\partial x} - D_{26}\frac{\partial \beta_\theta}{\partial x} - \frac{J'_{22}}{R}\frac{\partial \beta_\theta}{\partial \theta} - \frac{J'_{26}}{R}\frac{\partial \beta_x}{\partial \theta} = 0,$$

$$M_{\theta x} - B_{61}\frac{\partial u_x}{\partial x} - B_{66}\frac{\partial u_\theta}{\partial x} - \frac{H'_{62}}{R}\left(w + \frac{\partial u_\theta}{\partial \theta}\right) - \frac{H'_{66}}{R}\frac{\partial u_x}{\partial \theta} - D_{61}\frac{\partial \beta_x}{\partial x} - D_{66}\frac{\partial \beta_\theta}{\partial x} - \frac{J'_{62}}{R}\frac{\partial \beta_\theta}{\partial \theta} - \frac{J'_{66}}{R}\frac{\partial \beta_x}{\partial \theta} = 0,$$

$$Q_x - K_s G_{55}\left(\frac{\partial w}{\partial x} + \beta_x\right) + \frac{A_{54}}{R}\left(u_\theta - R\beta_\theta - \frac{\partial w}{\partial \theta}\right) = 0,$$

$$Q_\theta - A_{45}\left(\frac{\partial w}{\partial x} + \beta_x\right) + K_s\frac{G'_{44}}{R}\left(u_\theta - R\beta_\theta - \frac{\partial w}{\partial \theta}\right) = 0,$$

$$\frac{\partial N_{xx}}{\partial x} + \frac{1}{R}\frac{\partial N_{\theta x}}{\partial \theta} = -q_x, \qquad \frac{\partial N_{x\theta}}{\partial x} + \frac{1}{R}\frac{\partial N_{\theta\theta}}{\partial \theta} + \frac{Q_\theta}{R} = -q_\theta, \qquad \frac{\partial Q_x}{\partial x} + \frac{1}{R}\frac{\partial Q_\theta}{\partial \theta} + \frac{N_{\theta\theta}}{R} = q_x,$$

$$\frac{\partial M_{xx}}{\partial x} + \frac{1}{R}\frac{\partial M_{\theta x}}{\partial \theta} - Q_x = 0, \qquad \frac{\partial M_{x\theta}}{\partial x} + \frac{1}{R}\frac{\partial M_{\theta\theta}}{\partial \theta} - Q_\theta = 0,$$

Table 1. Governing equations for the system in Figure 1.

Here Q_i, N_{ij}, and M_{ij} represent shear and normal forces and moments, u_x, u_θ, w are the components of the displacement in cylindric coordinates, and β_x, β_θ are rotations of the tangents to the reference surface along the x and θ axis. We also denote by θ the counterclockwise orientation angle between the fiber direction and the panel coordinate system, and we set $m = \cos\theta$, $n = \sin\theta$. Other panel constants are

$$\begin{aligned}
&A_{ij} = \sum_{k=1}^{N} (\bar{Q}_{ij})_k (h_k - h_{k-1}), \quad B_{ij} = \tfrac{1}{2}\sum_{k=1}^{N} (\bar{Q}_{ij})_k (h_k^2 - h_{k-1}^2), \quad D_{ij} = \tfrac{1}{3}\sum_{k=1}^{N} (\bar{Q}_{ij})_k (h_k^3 - h_{k-1}^3),\\
&G_{ij} = A_{ij} + a_1 B_{ij} + a_2 D_{ij}, \qquad H_{ij} = B_{ij} + a_1 D_{ij} + a_2 E_{ij}, \qquad J_{ij} = D_{ij} + a_1 E_{ij} + a_2 F_{ij},\\
&G'_{ij} = A_{ij} + b_1 B_{ij} + b_2 D_{ij}, \qquad H'_{ij} = B_{ij} + b_1 D_{ij} + b_2 E_{ij}, \qquad J'_{ij} = D_{ij} + b_1 E_{ij} + b_2 F_{ij},
\end{aligned} \tag{1}$$

where for cylindrical panels $a_1 = b_1 = 1/R$, $a_2 = 0$, and $b_2 = 1/R^2$. Although some of their values are very small for the problems considered below, these coefficients are all preserved, to achieve better

accuracy and do justice to the capability of the differential cubature method. The $\bar{Q}_{ij}$ are defined as

$$\begin{aligned}
\bar{Q}_{11} &= Q_{11}m^4 + 2(Q_{12} + 2Q_{66})m^2n^2 + Q_{22}n^4,\\
\bar{Q}_{12} &= (Q_{11} + Q_{22} - 4Q_{66})m^2n^2 + Q_{12}(m^4 + n^4),\\
\bar{Q}_{22} &= Q_{11}n^4 + 2(Q_{12} + 2Q_{66})m^2n^2 + Q_{22}m^4,\\
\bar{Q}_{45} &= (Q_{55} - Q_{44})mn,\\
\bar{Q}_{16} &= (Q_{11} - Q_{12} - 2Q_{66})m^3n + (Q_{12} - Q_{22} + 2Q_{66})mn^3,\\
\bar{Q}_{26} &= (Q_{11} - Q_{12} - 2Q_{66})mn^3 + (Q_{12} - Q_{22} + 2Q_{66})m^3n,\\
\bar{Q}_{44} &= Q_{44}m^2 + Q_{55}n^2,\\
\bar{Q}_{55} &= Q_{44}n^2 + Q_{55}m^2,\\
\bar{Q}_{66} &= (Q_{11} + Q_{22} - 2Q_{12} - 2Q_{66})m^2n^2 + Q_{66}(m^4 + n^4),
\end{aligned} \tag{2}$$

while the Q_{ij} denote the elastic stiffness in the material coordinates (local axes) and are defined by

$$\begin{gathered}
Q_{11} = E_1/\Delta, \qquad Q_{12} = E_1\nu_{21}/\Delta, \qquad Q_{22} = E_2/\Delta, \qquad Q_{44} = G_{23},\\
Q_{55} = G_{13}, \qquad Q_{66} = G_{12}, \qquad \Delta = 1 - \nu_{12}\nu_{21},
\end{gathered} \tag{3}$$

where E_i, G_{ij} and ν_{ij} are, respectively, the Young's moduli of elasticity in the principal directions, the shear moduli of each lamina, and Poisson's ratios characterizing the transverse contraction (expansion) under tension (compression) in the directions of the coordinate axes.

The boundary conditions for the panel can be any combination of

$$\text{Free } (F): \quad \begin{cases} N_{xx} = N_{x\theta} = Q_x = M_{xx} = M_{x\theta} = 0 & \text{for } x \text{ constant},\\ N_{\theta x} = N_{\theta\theta} = Q_\theta = M_{\theta x} = M_{\theta\theta} = 0 & \text{for } \theta \text{ constant}; \end{cases} \tag{4}$$

$$\text{Simply supported } (S): \quad \begin{cases} N_{xx} = u_\theta = w = M_{xx} = \beta_\theta = 0 & \text{for } x \text{ constant},\\ u_x = N_{\theta\theta} = w = \beta_x = M_{\theta\theta} = 0 & \text{for } \theta \text{ constant}; \end{cases} \tag{5}$$

$$\text{Clamped } (C): \quad u_x = u_\theta = w = \beta_x = \beta_\theta = 0 \quad \text{for } x \text{ constant and for } \theta \text{ constant}. \tag{6}$$

Since there are ten derivatives in the fifteen equations, five boundary conditions is available and also enough in each edge.

3. Application of the DCM

The first step to apply the DCM is to form a nondimensional version of the governing equations in Table 1. To do so, we let q_0 be the uniform load or the amplitude of a sinusoidally distributed load, and introduce the dimensionless parameters

$$\begin{gathered}
w^* = w \times E_1h^3/q_0a^4, \qquad {u_i}^* = u_i \times E_1h^3/q_0a^4, \qquad {\beta_i}^* = \beta_i \times E_1h^3/q_0a^3,\\
{M_{ij}}^* = M_{ij}/q_0a^2, \qquad {N_{ij}}^* = N_{ij}/q_0a, \qquad {Q_i}^* = Q_i/q_0a,
\end{gathered} \tag{7}$$

where $i, j = 1, 2$. It is obvious that in the isotropic panel, E_1 in (7) should be replaced by E. Then, for instance, the first equation in Table 1 becomes

$$N_{xx}{}^* - G_{11}\frac{a^2}{E_1h^3}\frac{\partial u_x{}^*}{\partial x^*} - G_{16}\frac{a^2}{E_1h^3}\frac{\partial u_\theta{}^*}{\partial x^*} - \frac{A_{12}}{R}\frac{a^3}{E_1h^3}\left(w + \frac{\partial u_\theta}{\partial \theta}\right) - \frac{A_{16}}{R}\frac{a^3}{E_1h^3}\frac{\partial u_x}{\partial \theta}$$
$$- H_{11}\frac{a}{E_1h^3}\frac{\partial \beta_x}{\partial x^*} - H_{16}\frac{a}{E_1h^3}\frac{\partial \beta_\theta{}^*}{\partial x^*} - \frac{B_{12}}{R}\frac{a^2}{E_1h^3}\frac{\partial \beta_\theta{}^*}{\partial \theta} - \frac{B_{16}}{R}\frac{a^2}{E_1h^3}\frac{\partial \beta_x{}^*}{\partial \theta} = 0. \quad (8)$$

The next step is to choose a grid for the panel domain. A particular procedure should be used for node generation and their numbering in the DCM; details are given in [Civan 1994; Liew and Liu 1997; 1998; Teo and Liew 2002; Wu and Liu 2005]. For example, Figure 2 shows the entire panel with 61 nodes and their numbers. This method for grid generation and node numbering minimizes computational efforts. For other kinds of structures such as rectangular panel, the same numbering pattern for square panel is used in a scaled format.

It is then necessary to discretize the dimensionless governing equations. In the DCM, any linear operation such as a continuous function or various orders of partial derivatives of a multivariable function can be expressed as a weighted linear sum of discrete functions chosen within the overall domain of the problem [Civan 1994]. For instance, in a two-dimensional problem, the cubature approximation at the i-th discrete node is given by

$$\Re\{f(x, y)\}_i \cong \sum_{j=1}^{n} c_{ij} f(x_j, y_j) \quad i = 1, 2, \ldots, n, \quad (9)$$

where $\Re$ denotes a linear differential operator which can be any order of partial derivatives or combinations of these partial derivatives, i is the index of arbitrarily sequenced grid points for the two-dimensional solution domain, n is the total number of discrete points within the domain, and the c_{ij} are the $n \times n$

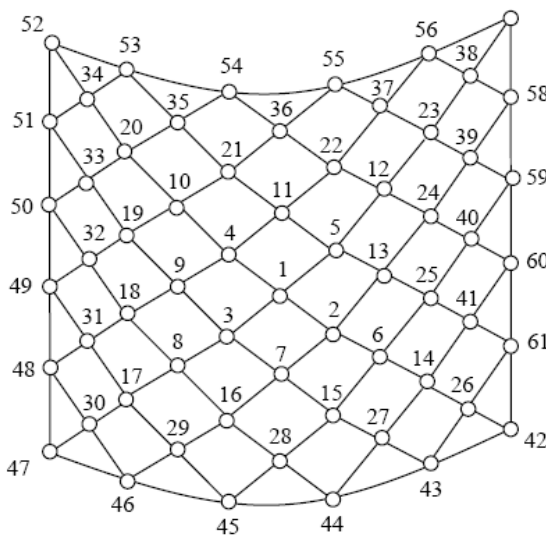

Figure 2. Grid generation and node numbering based on the DCM.

cubature weighting coefficients, to be determined. In order to find these coefficients, one uses a set of monomials in the form

$$F(x, y) = x^{m-n} y^n; \quad m = 0, 1, 2, \ldots, k-1; \quad n = 0, 1, 2, \ldots, m. \tag{10}$$

The number of these monomials should be equal to the total number n of grid points. The appropriate value of k in Equation (10) can be determined to satisfy this condition. For instance, for the case with 41 nodes, all of the monomials up to $k = 8$ should be used. However, for $k = 8$ there are only $k(k+1)/2 = 36$ monomials. Therefore, five more monomials from the value of $k = 9$ should be added to complete 41 monomials. The selection of these five monomials among those from $k = 9$ does not influence the results. Once the monomials in (10) are constructed, one can reach n equations by substituting these monomials into (9). Introducing the n equations obtained to all grid points leads to $n \times n$ equations, which are then used to calculate the $n \times n$ unknowns c_{ij} in (9).

This process should be done for all of the operators in the governing equations and boundary conditions if necessary. Having determined all the coefficients for the operators in the governing equations, one can substitute them according to (9) into the equations of Table 1 to reach a set of linear equations.

The last step is to apply boundary conditions to the main equations. As with other numerical methods, various techniques can be used for this purpose. In this study, the discretized forms of the boundary conditions are added to the main system of equations. This leads to an over-determined system, whose (approximate) solution is obtained using the least-squares method [Toorani and Lakis 2000].

4. Numerical results and discussions

The accuracy, convergence rate and performance of the presented DCM in obtaining solutions for the bending of laminated cylindrical panels are studied using seven test cases. Comparisons with results of other analytical and numerical studies available in the literature are provided in each case. To facilitate the comparison of our results with those in the literature, different definitions for dimensionless deflection of the panel are used in each case; the appropriate parameter definitions are mentioned both in the text and above the tables. Two kinds of loading conditions are used: uniform and sinusoidal distributed loads. To refer to the various boundary conditions, a number from 1 to 4 is assigned to each edge of the panel; see Figure 1. Thus, FSFC refers to a panel with free edges on the curved boundaries 1 and 3, simply supported on edge 2 and clamped on edge 4.

Case 1: SSSS panels with uniform loading. The first example is a SSSS cylindrical panel subjected to uniform loading q_0. Three types of panels are considered: isotropic, [0/90/0] and [0/90]. The panel is made of a square platform with side a. The ratio a/h of side length to thickness is chosen as 100, and the ration a/R of side length to radius as 0.5. The Poisson's ratio for the isotropic panel is 0.3, while the material properties of the orthotropic layers are taken from [Qatu and Algothani 1994]:

$$E_1/E_2 = 15.4, \qquad G_{12}/E_2 = 0.79, \qquad n_{12} = 0.3. \tag{11}$$

Table 2 reports the predictions of the DCM for dimensionless central deflection, moments, and forces as defined in (7). Only 81 nodes are used to reach final convergence for DCM. Included in the table are also results of analytical and finite element method reported in [Qatu and Algothani 1994]. It is

	Model	$10^3 w^*$	$10N_x^*$	$10N_\theta^*$	$10N_{x\theta}^*$	$10^3 M_x^*$	$10^3 M_\theta^*$	$10^3 M_{x\theta}^*$
Isotropic ($\nu = 0.3$)	Analytic	179	−278	−248	0	6	−13	0
	FEM	177	−274	−250	0	5	−12	0
	DCM	179.41	−278.49	−247.96	0.000708	5.7191	−13.079	0.0003283
[0/90/0]	Analytic	86	−214	−248	0	50	−19	0
	FEM	89	−215	−252	0	53	−15	0
	DCM	86.09	−214.37	−247.66	0.000558	50.26	−18.814	0.0001531
[0/90]	Analytic	110	−268	−247	0	−40	38	0
	FEM	109	−264	−247	0	−40	42	0
	DCM	110.54	−268.83	−246.79	0.000655	−40.122	37.551	0.0004902

Table 2. Dimensionless central deflection and stress resultants of SSSS cylindrical panels under uniform load. Analytic and FEM results from [Qatu and Algothani 1994].

seen from the table that the DCM predictions for deflection, forces and moments are much closer to the analytical results than those of the FEM, although the DCM computation used 81 grid points, versus 100 eight-node elements used in the FEM results.

Case 2: Symmetric SSSS panel under sinusoidal loading. This example deals with two kinds of symmetric cross-ply laminated cylindrical panels: [0/90/0] and [90/0/90]. The geometric parameters are length $a = 4$, total angle $\alpha = \pi/4$ and radius $R = 1$. The material properties of the layers are

$$E_1/E_2 = 25, \qquad G_{12}/E_2 = 0.5, \qquad G_{23}/E_2 = 0.2, \qquad \nu_{12} = 0.25 \tag{12}$$

and we use the sinusoidal loading condition

$$q = q_0 \sin\frac{\pi x}{a} \sin\frac{\pi\theta}{\alpha}. \tag{13}$$

The predictions of the presented model for normalized deflection of symmetric panels are tabulated in Table 3 for the [0/90/0] panel and in the top half of Table 4 for the [90/0/90] panel. For comparison, the table lists the normalized deflection $\overline{w}_1$ and the nondimensional deflection $\overline{w}_2$, defined by

$$\overline{w}_1 = 10wE_1/q_0 s^3, \qquad \overline{w}_2 = 10wE_1/q_0 R s^3; \qquad s = R/h. \tag{14}$$

	DCM			FEM
$s = R/h$	$n = 25$	$n = 41$	$n = 61$	[Reddy 2004]
50	0.2350	0.5458	0.5459	0.5458
100	0.1500	0.4718	0.4718	0.4718
500	0.0342	0.1028	0.1026	0.1028

Table 3. Normalized central deflection $\overline{w}_1 = 10wE_1/q_0 s^3$ of a [0/90/0] symmetric SSSS cylindrical panel under sinusoidal loading.

[90/0/90] unsymmetric pannel							
	DCM			FEM	FEM	TSDT	FSDT
$s = R/h$	$n = 25$	$n = 41$	$n = 61$	Bhaskar	Cheng	Reddy	Reddy
4	2.8742	3.7792	3.8197	4.0090	3.6067	4.0816	3.7990
10	0.6992	1.0589	1.0752	1.2230	1.2033	1.1835	1.0713
50	0.2350	0.5425	0.5459	0.5495	0.5486	0.5504	0.5457
100	0.1500	0.4702	0.4718	0.4715	0.4711	0.4727	0.4718
500	0.0342	0.1025	0.1026	0.1027	0.1027	0.1028	0.1028

[0/90] unsymmetric pannel							
	DCM			FEM	FEM	TSDT	FSDT
$s = R/h$	$n = 25$	$n = 41$	$n = 61$	Bhaskar	Cheng	Reddy	Reddy
4	4.7670	6.8671	6.9548	6.1000	5.0970	6.6698	7.3282
10	2.0527	3.4692	3.5066	3.3300	3.1658	3.4498	3.6715
50	0.1572	2.2558	2.2641	2.2420	2.2371	2.2627	2.2865
100	0.1718	1.3665	1.3737	1.3670	1.3667	1.3738	1.3781
500	0.0435	0.1007	0.1005	0.1005	0.1005	0.1006	0.1006

Table 4. Normalized central deflection $\overline{w}_2 = 10wE_1/q_0Rs^3$ of a [90/0/90] symmetric SSSS cylindrical panel (top) and a [0/90] unsymmetric SSSS cylindrical panel (bottom) under sinusoidal loading. The columns marked "Bhaskar", "Cheng" and "Reddy" are taken from [Bhaskar and Varadan 1991], [Cheng et al. 2000] and [Reddy and Arciniega 2004].

We validate the model with the FEM results from [Reddy 2004; Reddy and Arciniega 2004; Bhaskar and Varadan 1991], and the results from [Cheng et al. 2000], which are based on a new imperfect-interface model. Considering that the loading is nonuniform in this example, the agreement is encouraging: with only 61 grid points we get highly accurate predictions for deflection of the panel when compared with FEM. The results for [0/90/0] deviate by less than 0.2% from those obtained in [Reddy 2004], which is quite satisfactory.

Case 3: Unsymmetric SSSS panel under sinusoidal loading. Table 4, bottom, deals with the results for an unsymmetric panel under the same loading condition and having the same material and geometric properties as in case 2. The laminate arrangement is [0/90]. Verification is done with the results in [Reddy and Arciniega 2004; Bhaskar and Varadan 1991; Cheng et al. 2000], and the nondimensional deflection $\overline{w}_2$ defined in (14) is used. We see that even for an unsymmetric panel, the DCM provides acceptable predictions. For lower values of $s = R/h$, the DCM results are closer to the third-order shear deformation theory (TSDT) predictions.

Case 4: Symmetric panel with different boundary conditions. Next we consider a symmetric [0/90/0] cylindrical panel made from a square platform of side a, choosing the ratios $a/h = 10$ and $a/R = 0.2$.

	DCM					HSDT	CST
	$n=25$	$n=41$	$n=61$	$n=85$	$n=113$		
FSFS	6.8906	5.7138	5.7997	5.7910	5.8390	5.7912	5.5270
SSFS	3.4831	3.0705	3.2503	3.3308	3.3760	3.3519	3.1130
CSFS	1.3319	1.4614	1.5225	1.5490	1.5609	1.5809	1.1945
SSSS	0.8818	0.9428	0.9440	0.9440	0.9436	0.9650	0.7615
CSSS	0.5563	0.6103	0.6118	0.6119	0.6117	0.6337	0.3659
CSCS	0.3876	0.4346	0.4357	0.4357	0.4357	0.4540	0.2047

Table 5. Dimensionless central deflection $\overline{w}_3 = 100wE_2h^3/q_0a^4$ of [0/90/0] cylindrical panel with various boundary conditions under sinusoidal loading. Our DCM calculations are based on FSDT assumptions, while the comparison results, taken from [Bhaskar and Varadan 1991], are obtained using higher-order shear deformation theory (HSDT) and classical shell theory (CST).

The two straight edges of the panel are simply supported, while the curved edges can be free, simply supported or clamped. The panel is subjected to sinusoidal loading given by (13), and the material properties of the layers are

$$E_1 = 19.2\times10^6 \text{ psi}, \quad E_2 = 1.56\times10^6 \text{ psi}, \quad G_{12} = 0.82\times10^6 \text{ psi}, \quad G_{23} = 0.523\times10^6 \text{ psi}, \quad \nu_{12} = 0.24. \tag{15}$$

Comparison of the dimensionless central deflection of the panel with FEM [Bhaskar and Varadan 1991] is reported in Table 5. Following that paper, the dimensionless form of the deflection reported is $\overline{w}_3 = 100wE_2h^3/q_0a^4$.

Clearly the DCM results are closer to the HSDT predictions than the CST results. Furthermore, the results show rapid convergence of the method; only minor differences are observed between the predictions with 41 grid points and higher numbers.

Case 5: Unsymmetric panel with different boundary conditions. The next case differs from Case 4 only in that it deals with an unsymmetric [0/90] cylindrical panel. Table 6 presents the results for the dimensionless central deflection $\overline{w}_3 = 100wE_2h^3/q_0a^4$. The predictions are compared with the results of CST, FSDT and HSDT reported in [Khdeir et al. 1989]. We see that the FSDT results obtained by DCM are in very good agreement with FSDT predictions reported in that reference, with a discrepancy never exceeding 1.3%. The results for shells with free boundary condition show slightly higher discrepancy than those without free edges. For instance, in comparison with the FSDT results of [Khdeir et al. 1989], the differences for FSFS, SSFS and CSFS are 1.24%, 1.18%, and 0.95%, respectively, whereas for SSSS, CSSS, and CSCS they are 0.63%, 0.47%, and 0.35%.

Case 6: A symmetric SSSS angle-ply [θ/−θ/θ/−θ/θ] panel. The next example is a symmetric angle-ply $[\theta/-\theta/\theta/-\theta/\theta]$ cylindrical panel made of a square platform with side length of a. choosing the ratios $a/h = 10$ and $a/R = \frac{1}{3}$. All edges are simply supported and the transverse load is assumed to be uniform. The material properties of the layers are the same as in case 2; see (12).

Table 7 shows the predictions for the dimensionless central deflection $\overline{w}_3 = 100wE_2h^3/q_0a^4$ of the panel, for various orientation angles θ, together with FSDT- and HSDT-based results from [Bhaskar and

	DCM					CST	FSDT	HSDT
	$n=25$	$n=41$	$n=61$	$n=85$	$n=113$			
FSFS	3.1259	2.9997	2.9720	2.9483	2.9576	2.6933	2.9213	2.9061
SSFS	2.3134	2.3003	2.3033	2.3062	2.3170	2.1053	2.2899	2.2791
CSFS	1.2296	1.5853	1.6198	1.6288	1.6364	1.4163	1.6210	1.6154
SSSS	1.2361	1.5666	1.5712	1.5714	1.5712	1.4211	1.5614	1.5550
CSSS	0.7472	1.0911	1.0994	1.1000	1.1002	0.9221	1.0951	1.0914
CSCS	0.4304	0.7886	0.7964	0.7971	0.7974	0.6148	0.7946	0.7925

Table 6. Dimensionless central deflection $\overline{w}_3 = 100wE_2h^3/q_0a^4$ of [0/90] cylindrical panel with various boundary conditions under sinusoidal loading The comparison results on the right are taken from [Khdeir et al. 1989].

	DCM					HSDT	FSDT
	$n=25$	$n=41$	$n=61$	$n=85$	$n=113$		
$\theta=15°$	0.7896	0.8334	0.8481	0.8531	0.8552	0.8507	0.7802
$\theta=30°$	0.6179	0.7062	0.7233	0.7262	0.7199	0.7393	0.6386
$\theta=45°$	0.4516	0.5958	0.6234	0.6245	0.6471	0.6514	0.5561
$\theta=60°$	0.5781	0.7352	0.7421	0.7505	0.7516	0.7525	0.6517
$\theta=75°$	0.6181	0.8846	0.8812	0.8873	0.8893	0.8769	0.8053

Table 7. Dimensionless central deflection $\overline{w}_3 = 100wE_2h^3/q_0a^4$ of a $[\theta/-\theta/\theta/-\theta/\theta]$ SSSS cylindrical panel under uniform load. The comparison results are from [Bhaskar and Varadan 1991].

Varadan 1991]. It can be seen that discrepancies of the results for angle-ply laminated shells are higher than those of cross ply laminates.

Case 7: Symmetric* [0/90/0] *square plate under sinusoidal loading. The governing equations and solution procedure discussed here can also be employed for the bending analysis of rectangular plates, by making the panel radius R and the total angle α correspondingly small. If the dimensions of the plate are a and b, we take a as before and $\alpha = b/R$.

The last example includes a fully simply supported symmetric [0/90/0] square plate subjected to sinusoidal load; see Equation (13). Material properties of all layers are the same as (12). Predictions for the dimensionless central deflection $\overline{w}_4 = wE_2h^3/q_0a^4$ of the square plate are tabulated in Table 8. Again, comparisons with the results of analytical solutions [Whitney and Pagano 1970] and the generalized differential quadrature (GDQ) method [Aghdam et al. 2006] demonstrate good agreement. As can be concluded from the table, in the GDQ method results are obtained with 121 nodes while the DCM reaches the same level of accuracy by employing only 61 nodes. This might potentially mean that DCM requires less computation time than GDQ, for results of similar quality.

	DCM				GDQ 11×11	Analytic
a/h	$n = 13$	$n = 25$	$n = 41$	$n = 61$	Aghdam	Whitney
2	3.6450	5.2116	5.2288	5.2294	5.2293	5.2293
4	1.0174	1.7719	1.7750	1.7758	1.7758	1.7758
10	0.2086	0.6672	0.6683	0.6693	0.6693	0.6693
20	0.0556	0.4574	0.4923	0.4920	0.4921	0.4921
50	0.0021	0.1893	0.4406	0.4406	0.4411	0.4411
100	0.0001	0.1456	0.4310	0.4326	0.4337	0.4337

Table 8. Dimensionless central deflection $\overline{w}_4 = wE_2h^3/q_0a^4$ of an SSSS [0/90/0] square plate under sinusoidal loading. The columns marked "Aghdam" and "Whitney" are taken from [Aghdam et al. 2006] and [Whitney and Pagano 1970].

5. Conclusion

We studied the performance of the differential cubature method in the static analysis of laminated cylindrical panels subject to uniform and sinusoidal loadings. The formulation presented allows the treatment of any type of lamination, whether symmetric or unsymmetric, and any combination of clamped, simply supported and free boundary conditions on the edges. Starting from the governing equations for cylindrical panels based on first-order shear deformation theory (fifteen first-order partial differential equations in the same number of unknowns), we proceed by discretizing the solution domain, governing equations and related boundary conditions, according to the DCM procedure. The results show that DCM can provide reasonably accurate predictions with relatively few grid points, and so may require less computational time than other numerical techniques, for a given accuracy level. The method provides the same order of accuracy for all stress and displacement variables within the solution domain. Comparison of calculated stress resultants and displacement components shows good agreement with results obtained using other analytical and numerical techniques.

List of symbols

R	radius	a	side length
h	thickness	s	radius–to–thickness ratio
α	total angle (Figure 1)	q_0	uniform load or the maximum of sinusoidally distributed load
θ	orientation angle		
N_{ij}	normal force	Q_i	shear force
u_x, u_θ, w	displacement components	M_{ij}	moment
Q_{ij}	elastic stiffness in the material coordinates (local axes)	β_x, β_θ	rotations of the tangents
		E_i	Young's moduli
G_{ij}	shear moduli	ν_{ij}	Poisson's ratios
$\overline{w}_1$	normalized deflection	$\overline{w}_2$	nondimension deflection
w^*, ${u_i}^*$, ${\beta_i}^*$	dimensionless parameters	${M_{ij}}^*$, ${N_{ij}}^*$, ${Q_i}^*$	dimensionless parameters

References

[Aghdam et al. 2006] M. M. Aghdam, M. R. N. Farahani, M. Dashty, and S. M. Rezaei Niya, "Application of generalized differential quadrature method to the bending of thick laminated plates with various boundary conditions", *Appl. Mech. Mater.* **5–6** (2006), 407–414.

[Alavi et al. 2006] S. M. Alavi, M. M. Aghdam, and A. Eftekhari, "Three-dimensional elasticity analysis of thick rectangular laminated composite plates using meshless local Petrov-Galerkin (MLPG) method", *Appl. Mech. Mater.* **5–6** (2006), 331–338.

[Alijani et al. 2008] F. Alijani, M. M. Aghdam, and M. Abouhamze, "Application of the extended Kantorovich method to the bending of clamped cylindrical panels", *Eur. J. Mech. A Solids* **27**:3 (2008), 378–388.

[Artioli et al. 2005] E. Artioli, P. L. Gould, and E. Viola, "A differential quadrature method solution for shear-deformable shells of revolution", *Eng. Struct.* **27**:13 (2005), 1879–1892.

[Berghaus 2001] D. G. Berghaus, *Numerical methods for experimental mechanics*, Kluwer, Boston, 2001.

[Bhaskar and Varadan 1991] K. Bhaskar and T. K. Varadan, "A higher-order theory for bending analysis of laminated shells of revolution", *Comput. Struct.* **40**:4 (1991), 815–819.

[Cheng et al. 2000] Z. Q. Cheng, L. H. He, and S. Kitipornchai, "Influence of imperfect interfaces on bending and vibration of laminated composite shells", *Int. J. Solids Struct.* **37**:15 (2000), 2127–2150.

[Civan 1994] F. Civan, "Solving multivariable mathematical models by the quadrature and cubature methods", *Numer. Meth. Partial Differential Eq.* **10**:5 (1994), 545–567.

[Jianqiao 1988] Y. Jianqiao, "A new approach for the bending problem of shallow shell by the boundary element method", *Appl. Math. Model.* **12**:5 (1988), 467–470.

[Khdeir et al. 1989] A. A. Khdeir, L. Librescu, and D. Frederick, "A shear deformable theory of laminated composite shallow shell-type panels and their response analysis, II: static response", *Acta Mech.* **77**:1-2 (1989), l–12.

[Liew and Liu 1997] K. M. Liew and F. L. Liu, "Differential cubature method: a solution technique for Kirchhoff plates of arbitrary shape", *Comput. Methods Appl. Mech. Eng.* **145**:1-2 (1997), 1–10.

[Liu and Liew 1998] F. L. Liu and K. M. Liew, "Differential cubature method for static solutions of arbitrarily shaped thick plates", *Int. J. Solids Struct.* **35**:28–29 (1998), 3655–3674.

[Qatu and Algothani 1994] M. S. Qatu and A. Algothani, "Bending analysis of laminated plates and shells by different methods", *Comput. Struct.* **52**:3 (1994), 529–539.

[Ramesh and Krishnamoorthy 1995] G. Ramesh and C. S. Krishnamoorthy, "Geometrically non-linear analysis of plates and shallow shells by dynamic relaxation", *Comput. Methods Appl. Mech. Eng.* **123**:1-4 (1995), 15–32.

[Reddy 2004] J. N. Reddy, *Mechanics of laminated composite plates and shells: theory and analysis*, 2nd ed., CRC Press, Boca Raton, FL, 2004.

[Reddy and Arciniega 2004] J. N. Reddy and R. A. Arciniega, "Shear deformation plate and shell theories: from Stavsky to present", *Mech. Adv. Mater. Struct.* **11**:6 (2004), 535–582.

[Smith 2000] T. A. Smith, "Finite difference analysis of rotationally symmetric shells using variable node point spacings", *J. Sound Vib.* **230**:5 (2000), 1119–1145.

[Teo and Liew 2002] T. M. Teo and K. M. Liew, "Differential cubature method for analysis of shear deformable rectangular plates on Pasternak foundations", *Int. J. Mech. Sci.* **44**:6 (2002), 1179–1194.

[Toorani and Lakis 2000] M. H. Toorani and A. A. Lakis, "General equations of anisotropic plates and shells including transverse shear deformations, rotary inertia and initial curvature effects", *J. Sound Vib.* **237**:4 (2000), 561–615.

[Toorani and Lakis 2001] M. H. Toorani and A. A. Lakis, "Shear deformation in dynamic analysis of anisotropic laminated open cylindrical shells filled with or subjected to a flowing fluid", *Comput. Methods Appl. Mech. Eng.* **190**:37-38 (2001), 4929–4966.

[Whitney and Pagano 1970] J. M. Whitney and N. J. Pagano, "Shear deformation in heterogeneous anisotropic plates", *J. Appl. Mech.* (*ASME*) **37**:4 (1970), 1031–6.

[Wu and Liu 2005] L. Wu and J. Liu, "Free vibration analysis of arbitrary shaped thick plates by differential cubature method", *Int. J. Mech. Sci.* **47**:1 (2005), 63–81.

[Yuan et al. 1998] S. Yuan, Y. Jin, and F. W. Williams, "Bending analysis of Mindlin plates by extended Kantorovich method", *J. Eng. Mech.* (*ASCE*) **124**:12 (1998), 1339–1345.

Received 12 Oct 2008. Revised 21 Mar 2009. Accepted 25 Mar 2009.

S. MAHMOUD MOUSAVI: s_mousavi@aut.ac.ir
Department of Mechanical Engineering, Amirkabir University of Technology, 424 Hafez Avenue, Tehran 15875–4413, Iran

MOHAMAD M. AGHDAM: semahmoudmousavi@yahoo.com
Department of Mechanical Engineering, Amirkabir University of Technology, 424 Hafez Avenue, Tehran 15875–4413, Iran